



Determination of tensile strength in soils as a geotechnical design parameter through correlations using numerical models

Determinación de la resistencia a la tracción en suelos como parámetro de diseño geotécnico a través de correlaciones con el uso de modelos numéricos

Johannes Enrique Briceño Balza^{1*}, Norly Thairis Belandria Rodríguez², Francisco León Oviedo³

Highlights

- A compression–tension correlation was established for predominantly sandy soils.
- Tensile strength ranged between 17% and 19% of unconfined compressive strength.
- Numerical modeling was used to assess the indirect estimation of soil tensile strength.

Innovaciencia

ISSN: 2346-075X

E- ISSN: 2346-075X

Innovaciencia 2026; 14(1): e5919

<http://dx.doi.org/10.15649/2346075X.5919>

ORIGINAL RESEARCH

How to cite this article:

Briceño Balza JE, Belandria Rodríguez NT, León Oviedo F. Determination of tensile strength in soils as a geotechnical design parameter through correlations using numerical models. *Innovaciencia*. 2026;14(1): e 5919.

<http://dx.doi.org/10.15649/2346075X.5919>

Received: 18 November 2025

Accepted: 23 April 2026

Published: 15 May 2026

Keywords:

Soil tensile strength; compressive strength; indirect tensile test; compression–tension correlation; numerical modeling.

Palabras clave:

Resistencia a tracción en suelos; resistencia a compresión; ensayo de tracción indirecta; correlación compresión–tracción; modelación numérica.

ABSTRACT

Introduction. Tensile cracking can affect the stability and performance of geotechnical structures, particularly when tensile failure mechanisms develop in soil masses. **Objective.** To establish a correlation between σ_c and σ_t in soils through laboratory testing and numerical modeling. **Materials and Methods.** Unconfined compression and indirect tensile tests were conducted on three predominantly sandy soils with different fines contents. Numerical simulations were performed to reproduce the stress conditions of both tests, and statistical analyses were applied to evaluate the relationship between σ_c and σ_t . **Results.** Tensile strength (σ_t) was significantly lower than compressive strength (σ_c), ranging between 17% and 19% of σ_c . A positive linear relationship was identified between both parameters, with high correlation and determination coefficients. Numerical simulations showed good agreement with experimental data. **Conclusions.** A correlation equation between σ_c and σ_t is proposed for the analyzed soils, allowing the indirect estimation of tensile strength from compressive strength values. Its applicability is limited to soils with characteristics similar to those studied.

RESUMEN

Introducción. La formación de grietas por tracción puede afectar la estabilidad y el desempeño de estructuras geotécnicas, particularmente cuando se desarrollan mecanismos de falla por tracción en masas de suelo. **Objetivo.** Establecer una correlación entre la resistencia a compresión (σ_c) y la resistencia a tracción (σ_t) en suelos, basada en ensayos de laboratorio y modelación numérica. **Materiales y métodos.** Se realizaron ensayos de compresión simple y tracción indirecta en tres suelos predominantemente arenosos con diferentes contenidos de finos. Adicionalmente, se llevaron a cabo simulaciones numéricas para reproducir las condiciones de esfuerzo de ambos ensayos, y se aplicaron análisis estadísticos para evaluar la relación entre σ_c y σ_t . **Resultados.** La resistencia a tracción (σ_t) fue significativamente menor que la resistencia a compresión (σ_c), con valores entre el 17% y el 19% de σ_c . Se identificó una relación lineal positiva entre ambos parámetros, con altos coeficientes de correlación y determinación. Las simulaciones numéricas mostraron buena concordancia con los datos experimentales. **Conclusiones.** Se propone una ecuación de correlación entre σ_c y σ_t para los valores analizados, que permite estimar indirectamente la resistencia a tracción a partir de valores de resistencia a compresión. Su aplicabilidad se limita a suelos con características similares a los estudiados.



- 1 Department of Roads, School of Civil Engineering, Faculty of Engineering, Universidad de Los Andes. Merida, Venezuela. *Corresponding author: ✉ ingjebb@gmail.com; johannes@ula.ve
- 2 Applied Geology Research Group (AGRG), School of Geological Engineering, Faculty of Engineering, Universidad de Los Andes. Merida, Venezuela. norlyb@gmail.com
- 3 Mechanical Vibrations Laboratory, School of Mechanical Engineering, Faculty of Engineering, Universidad de Los Andes. Merida, Venezuela. fleon@ula.ve

Open access

INTRODUCTION

Because the tensile strength of soils (σ_t) is low compared to their compressive strength (σ_c), it is often neglected in the development of geotechnical methods and studies. However, in recent geotechnical applications, well-established reinforcement methods used in concrete have been adopted to improve the mechanical (strength) and elastic properties of materials such as soils and asphalt mixtures. These methods include the incorporation of reinforcements such as natural and synthetic fibers, as well as polypropylene macrofibers and microfibers^(1–5), primarily to increase σ_t , thereby reducing failures and associated effects, such as the initiation and propagation of tensile cracks. In specific cases, σ_t must be explicitly considered⁽⁶⁾. One such case is slope stability involving tension cracks. Prior to a landslide, structures may exhibit multiple fissures, foundation settlement, and cracks on the slope surface that develop rapidly⁽⁷⁾. The evolution of landslides has been closely linked to the development of tension cracks⁽⁸⁾. In engineering practice, it has been observed that, before failure, cracks tend to appear in the upper part of embankments or slopes. These cracks allow rainwater infiltration, increasing lateral tensile stresses and destabilizing effects. Current slope stability analysis methods may therefore require revision, as the most critical conditions arise when tension cracks are considered⁽⁹⁾. Not only shear stresses but also tensile stresses—which cannot be disregarded—contribute to the formation of the failure surface and the development of tension cracks. Furthermore, tension cracks have been identified as a significant issue for slope stability⁽¹⁰⁾.

The presence of tension cracks significantly increases the stresses within the soil mass and, consequently, slope instability⁽¹¹⁾. The tensile strength σ_t is commonly explained in terms of interparticle cohesion, which can be divided into real and apparent cohesion, based on conventional tests and analytical developments, although no explicit expression for σ_t is provided⁽¹²⁾. In contrast, σ_t has been estimated by relating it to the uniaxial compressive strength, thereby simplifying testing procedures⁽¹³⁾. Similarly, σ_t has been assessed indirectly using uniaxial compression testing equipment⁽¹⁴⁾. To assess σ_t , both direct and indirect testing methods have been employed. Direct methods require complex laboratory equipment available in very few facilities, whereas indirect methods provide an alternative means for estimating this parameter. Direct testing methods typically involve pneumatic suction techniques to generate vacuum conditions and induce tensile failure. Given the difficulty of directly measuring σ_t , an alternative approach involves laboratory tests in which tensile stresses are applied indirectly using equipment commonly available in soil mechanics laboratories. This involves indirect compression or tensile tests to estimate σ_t . Another approach consists of employing numerical methods, which are widely used in geotechnical engineering^(15–17), to simulate these tests and establish the required correlations. The comparison of the mechanical and hydraulic behavior of soils in applied geotechnics—based on laboratory and field tests (traditional and/or conventional methods)—with results obtained from numerical models has become increasingly common in recent years, with extensive supporting literature available⁽¹⁸⁾. Likewise, correlations of geotechnical parameters based on physical laboratory or field tests have been widely reported^(19–20). However, the estimation of soil mechanical or hydraulic properties through an integrated experimental–numerical approach remains underdeveloped. Therefore, to provide novel, rapid, and reliable tools for geotechnical analysis, this study addresses the following research questions: Are the values of σ_c and σ_t

obtained from laboratory tests comparable to those derived from numerical modeling? Is it possible to establish a reliable correlation between σ_c and σ_t ?

To address these questions, and to incorporate σ_t (structural strength) into geotechnical analysis, this study proposes the use of the unconfined compression test and the indirect tensile test. This approach enables the establishment of correlations between compressive and tensile stresses for certain soils. The laboratory results, once the mechanical behavior of the soil has been characterized, can be modeled to validate the compression–tension relationship and extend its applicability to other soil types. The main scientific contribution of this study lies in the development of correlation equations between σ_c and σ_t for the analyzed soils, based on both experimental testing and numerical modeling within a deterministic framework. This demonstrates the feasibility of an experimental–numerical approach for characterizing soil behavior. Furthermore, a general procedure is proposed for establishing such correlations in soils with characteristics and properties different from those considered in this study.

MATERIALS AND METHODS

Samples

To obtain a representative range of soils, samples were collected from three locations in Mérida State, Venezuela: two in the Libertador municipality and one in the Sucre municipality. The selected sites were Alto Prado Sector, Pie del Tiro Sector, and Lagunillas. (Table 1) presents the sampling locations, as well as the mechanical and elastic properties of the soils.

Table 1. Sample location and mechanical and elastic properties of the soil

Sample	1	2	3
Location	Alto Prado	Pie del Tiro	Lagunillas
Particle size test			
G (%)	0.00	0.00	24.71
S (%)	53.86	61.22	54.12
F (%)	46.15	38.78	21.71
Consistency limits			
ω_l (%)	26.63	25.06	21.09
ω_p (%)	22.57	19.88	14.48
PI (%)	4.06	5.18	6.61
USCS	SM	SC	SC
ω (%)	11.00	11.00	7.00
γ_h (lb/in ³)	7.26x10 ⁻²	7.07x10 ⁻²	7.21x10 ⁻²
C (lb/in ²)	3.21	2.77	4.08
\emptyset (°)	34.00	31.00	31.00
E (lb/in ²)	2000.00	2000.00	2000.00
ν	0.35	0.35	0.35

* G: percentage of gravel, S: percentage of sand, F: percentage of fines, ω_l : liquid limit, ω_p : plastic limit, PI: plastic index, USCS: unified soil classification system, ω : moisture content, γ_h : wet unit weight, C: cohesion of the material, \emptyset : angle of internal friction, E: modulus of elasticity, ν : Poisson's ratio, respectively

Experimental and Numerical Program

This study combined experimental testing and numerical modeling to evaluate the behavior of soils under tensile and compressive stress conditions. Laboratory tests were used to obtain strength and elastic properties, while numerical simulations were performed to reproduce the stress states of the specimens and support the development of correlations between tensile strength and unconfined compressive strength.

Experimental evaluation of soil behavior under tensile and compressive stresses

A total of sixty (60) specimens were prepared for each soil type. Standard characterization tests were conducted to determine mechanical and elastic properties, including unit weight, specific gravity, moisture content, grain size distribution, and consistency limits. Soil classification was performed according to the Unified Soil Classification System (USCS). Unconfined compression tests were carried out to obtain the compressive strength (σ_c), while indirect tensile tests were performed to estimate the tensile strength (σ_t).

Statistical analysis

The statistical analysis was performed to evaluate the relationship between compressive strength (σ_c) and tensile strength (σ_t). First, data normality was assessed using the Kolmogorov–Smirnov test at a significance level of $\alpha = 0.05$. Pearson's linear correlation coefficient (r_{xy}) was then calculated analytically and using R-Studio for each soil sample and for the combined dataset. Finally, the coefficient of determination (R^2) was obtained to quantify the proportion of shared variability between σ_c and σ_t .

Numerical modeling of soil behavior

In geotechnical engineering, the Mohr–Coulomb failure criterion is widely used to represent soil behavior, assuming an elastoplastic response. This criterion describes shear strength as a function of cohesion (C) and the angle of internal friction (ϕ), and defines failure when the shear stress (τ) reaches the shear strength of the material^(21–23). The Finite Element Method (FEM) enables the analysis of stress–strain behavior under complex conditions and is commonly applied in geotechnical problems where traditional methods, such as the Limit Equilibrium Method (LEM), present limitations. Applications include slope stability and foundation analysis. In this study, the Mohr–Coulomb failure criterion and FEM were adopted as the primary modeling tools^(24–25). A cylindrical specimen was modeled using the commercial software Abaqus 6.13, based on FEM. The mechanical and elastic properties obtained from laboratory tests were assigned to the model. An elastoplastic Mohr–Coulomb constitutive model was defined, along with the corresponding analysis steps and increments. The model was discretized through meshing, and appropriate boundary conditions were applied. Loads were then imposed to reproduce the stress states of the laboratory tests, allowing the determination of compressive and tensile failure stresses, corresponding to σ_c and σ_t , respectively.

Unconfined compression test model

The numerical model was subjected to stress conditions equivalent to those of the unconfined compression test, where the minor principal stress was zero ($\sigma_3 = 0$) and the major principal stress corresponded to the compressive strength ($\sigma_1 = \sigma_c$). For all samples, the cylindrical specimen used in the model had a diameter of

2.07 in and a height of 4.07 in. The simulation results were obtained as contour plots (color maps), from which the compressive strength ($\sigma_1 = \sigma_c$) was determined.

Indirect tensile test model

The model was subjected to stress conditions equivalent to those of the indirect tensile test, where the major principal stress was zero ($\sigma_1 = 0$) and the minor principal stress corresponded to the tensile strength ($\sigma_3 = \sigma_t$). For all samples, the cylindrical specimen used in the model had a diameter of 2.067 in and a height of 2.370 in. From the numerical results, the stress distribution was obtained, and σ_3 was determined through parametric relationships, corresponding to the tensile strength (σ_t).

Correlation between tensile and compressive strength

Soil behavior under tensile and compressive stresses was evaluated through laboratory testing and numerical simulation. After performing unconfined compression and indirect tensile tests on the sixty (60) specimens for each soil type, and completing the corresponding simulations, σ_c - σ_t relationships were established for each material. Based on these results, correlation equations between tensile and compressive strengths were developed.

RESULTS

Experimental strength results

The compressive strength (σ_c) and tensile strength (σ_t) were obtained from sixty (60) specimens tested for each soil sample. The average values obtained from the laboratory tests are presented in (Table 2).

Table 2. Compressive and tensile strength of soil (average values determined in the laboratory).

Sample	σ_c (kg/cm ²)/(lb/in ²) Average	σ_t (kg/cm ²)/(lb/in ²) average	$\sigma_t = \% \sigma_c$	Standard deviation (σ_c)	Standard deviation (σ_t)
1	1.628 / 23.156	-0.288 / -4.096	17.68	0.037	0.008
2	1.284 / 18.263	-0.221 / -3.143	17.21	0.030	0.006
3	1.596 / 22.701	-0.291 / -4.139	18.19	0.035	0.007

The relationship between compressive strength and tensile strength for the different soil materials is shown in (Figure 1). Based on the evaluation of different trend options, a linear trend line was selected as the best fit to the observed behavior. Equation (1) presents the correlation between σ_c and σ_t for samples 1, 2, and 3, with a coefficient of determination of $R^2 = 0.9794$. This correlation allows tensile strength to be estimated from compressive strength for soils with similar characteristics, enabling its consideration in geotechnical analyses.

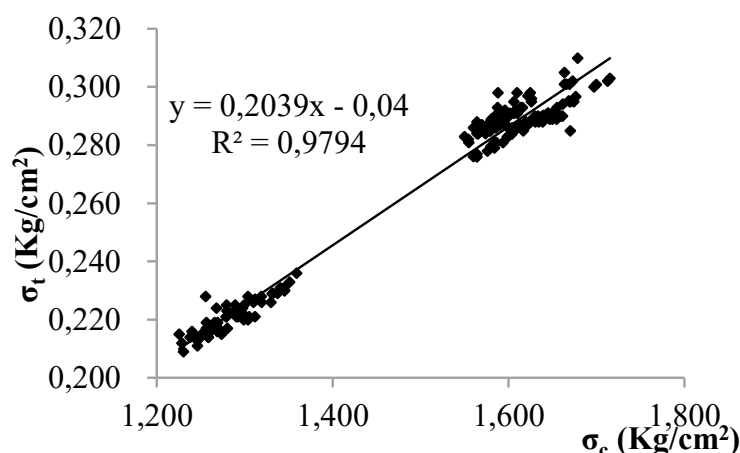


Figure 1. Relationship between compressive strength (σ_c) and tensile strength (σ_t) for samples 1, 2, and 3.

$$\text{Equation 1} \quad \sigma_t = -(0.2059 \sigma_c + 0.04)$$

Statistical correlation analysis (σ_c – σ_t)

The normality analysis showed different distribution patterns among the soil samples and the grouped dataset, as summarized in (Table 3). Pearson's correlation coefficients between σ_c and σ_t were then calculated for each sample and for the combined dataset, with the results presented in (Table 4). The corresponding coefficients of determination (R^2), used to quantify the proportion of shared variability between both variables, are shown in (Table 5).

Table 3. Normality analysis using the Kolmogorov–Smirnov test (σ_c and σ_t)

Sample	1	2	3	1,2, and 3
$p\text{-valor}(\sigma_c)$	0.96810	0.20530	0.00159	2.2×10^{-16}
$p\text{-valor}(\sigma_t)$	0.02632	0.06417	0.00023	2.2×10^{-16}

Table 4. Pearson's linear correlation coefficient between σ_c and σ_t

Sample	1	2	3	1, 2, and 3
N	60	60	60	180
X	1.6283	1.2844	1.5964	1.5030
\bar{Y}	0.2881	0.2211	0.2905	0.2666
S_x	0.0368	0.0345	0.0299	0.1588
S_y	0.0059	0.0062	0,0059	0.0327
r_{xy} (1)	0.9257	0.8984	0.9145	0.9896
r_{xy} (2)	1.0000	0.9999	1.0000	0.9997
r_{xy} (3)	0.9257	0.8985	0.9144	0.9896
t	18.633	15.583	17.213	91.221
$p\text{-valor}$	$<2.2 \times 10^{-16}$	$<2.2 \times 10^{-16}$	$<2.2 \times 10^{-16}$	$<2.2 \times 10^{-16}$
α	0.05	0.05	0.05	0.05

*N: sample size, X: arithmetic mean of compressive strength, \bar{Y} : arithmetic mean of tensile strength, S_x : standard deviation of compressive strength, S_y : standard deviation of tensile strength, r_{xy} (1): Pearson's linear correlation coefficient (direct scores), r_{xy} (2): Pearson's linear correlation coefficient (differential scores), r_{xy} (3): Pearson's linear correlation coefficient (standardized scores), t: test statistic for the rejection region, p-value: area to the right of the test statistic, α : level of significance (error).

Table 5. Coefficient of determination (R^2) between σ_c and σ_t

Sample	R^2 (1)	R^2 (2)	R^2 (3)
1	0.8569	0.9999	0.8569
2	0.8073	0.9998	0.8073
3	0.8362	0.9999	0.8362
1,2, and 3	0.9794	0.9994	0.9794

Numerical modeling results

Unconfined compression test model

The numerical simulation results for sample 1, including the applied loads, mesh discretization, and resulting stress distribution, are presented in (Figure 2).

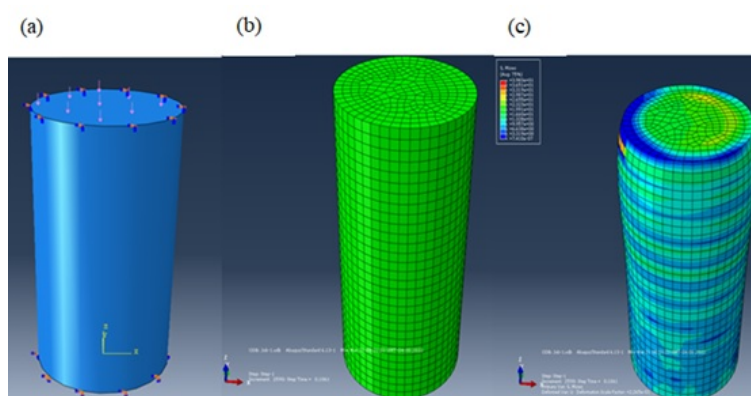


Figure 2. (a) Applied loads ($\sigma_3 = 0, \sigma_1 = \sigma_c$); (b) mesh discretization; (c) resulting stresses. Unconfined compression test, Sample 1 (Abaqus 6.13).

Indirect tensile test model

The numerical simulation results for sample 1 under indirect tensile conditions include the applied loads, mesh discretization, and resulting stress distribution, as shown in (Figure 3).

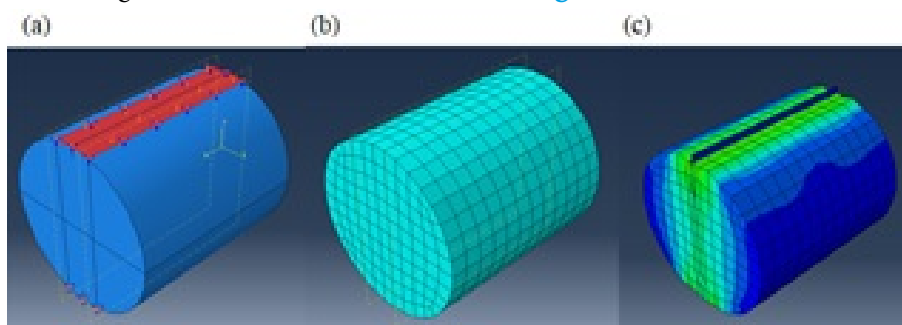


Figure 3. (a) Applied loads ($\sigma_3 = \sigma_t, \sigma_1 = 0$); (b) mesh discretization; (c) resulting stresses. Indirect tensile test, Sample 1 (Abaqus 6.13).

Comparison between laboratory and simulation results

After performing the simulations using the commercial modeling program, the compressive strength (σ_c) and tensile strength (σ_t) obtained from both laboratory tests and numerical simulations are presented in

(Table 6). Additional simulations were conducted under triaxial stress conditions for comparison purposes. For compressive strength, $\sigma_3 = 0$ and $\sigma_1 = \sigma_c$ were applied, whereas for tensile strength, $\sigma_1 = 0$ and $\sigma_3 = \sigma_t$ were considered.

Table 6. Compressive and tensile strengths obtained from laboratory tests and numerical simulations

Sample	Mode	σ_c (kg/cm ²)	σ_c (lb/in ²)	σ_t (kg/cm ²)	σ_t (lb/in ²)	$\sigma_t = \% \sigma_c$
1	Laboratory	1.628	23.156	-0.288	-4.096	17.68
	Simulation	1.633	23.230	-0.288	-4.096	17.63

DISCUSSION

The soils analyzed are predominantly sandy, with the presence of silt and clay fractions. The specimens were prepared at a moisture content that allowed the formation of tensile cracks to be visually identified during the indirect tensile test. Regarding the results, (Table 6) shows that tensile strength is significantly lower than compressive strength, with σ_t ranging between 17% and 19% of σ_c . This proportion is consistent across all analyzed samples. The normality analysis (Table 3) indicates that, in most cases, the p -value is lower than the significance level ($\alpha = 0.05$), leading to the rejection of the null hypothesis (H_0). Therefore, the data do not follow a normal distribution. This behavior is more evident when all samples are considered together to establish a single correlation. The scatter plot in (Figure 1), corresponding to the combined dataset, shows a positive linear relationship between σ_c and σ_t , although with some dispersion. This indicates that the relationship is not perfectly linear, as some values deviate from the fitted trend. To quantify this relationship, Pearson's linear correlation coefficient (r_{xy}) was used. The results presented in (Table 4), show values greater than 0.9, indicating a strong linear relationship between σ_c and σ_t . Additionally, in all cases, the p -values are lower than the significance level ($\alpha = 0.05$), leading to the rejection of the null hypothesis ($r_{xy} = 0$) and confirming that the variables are linearly related. The coefficient of determination (R^2) further supports this relationship, indicating that a high proportion of the variability in σ_t can be explained by σ_c . As shown in (Table 5), high R^2 values are obtained both for individual samples and for the combined dataset. Based on these results, a single correlation between compressive strength (σ_c) and tensile strength (σ_t) can be established using the combined dataset of the three soil samples. This relationship is represented by Equation (1) and (Figure 1). The observed proportion between σ_t and σ_c (17–19%) reflects the mechanical response of the analyzed soils and provides a consistent basis for interpreting their behavior.

In this context, tensile strength in soils is generally much smaller than compressive strength and plays a key role in crack initiation and propagation⁽²⁶⁻²⁷⁾. However, its determination remains challenging, as no consensus exists regarding the most suitable testing method, and different experimental approaches may lead to significantly different results⁽²⁸⁾. Conventional methods, such as direct tensile tests and Brazilian tests, present limitations related to stress distribution, specimen preparation, and loading conditions, which can influence the measured tensile strength values⁽²⁷⁻²⁸⁾. In addition, tensile strength has been shown to be strongly influenced by factors such

as water content, soil microstructure, and deformation behavior, contributing to its variability⁽²⁶⁾. Therefore, σ_t is not only dependent on soil properties but also on the testing methodology adopted, any relationship between σ_t and σ_c should be interpreted within the context of the material characteristics, testing methodology, and experimental conditions considered in each study. The comparison between laboratory and numerical results (**Table 6**) shows a close agreement between both approaches, with differences that are small relative to the magnitude of the measured values.

Finally, it should be noted that the differences between the analyzed materials are relatively small and do not significantly affect the proposed correlation for geotechnical applications. However, the applicability of the proposed σ_c – σ_t correlation is limited to soils with characteristics similar to those analyzed in this study. Since only three predominantly sandy soils with different fines contents were evaluated, additional tests on soils with different gradations, plasticity levels, moisture conditions, and densities are required to extend the scope of the correlation. Furthermore, the numerical results are influenced by the assumptions of the adopted constitutive model; therefore, the proposed procedure should be validated under other soil types and testing conditions before being generalized. These aspects are consistent with the variability reported in the literature and reinforce the need to interpret the proposed correlation within its specific experimental framework.

CONCLUSIONS

Laboratory testing allowed the determination of compressive strength (σ_c) and tensile strength (σ_t) for the analyzed soils. The results confirm that tensile strength is significantly lower than compressive strength, although it becomes relevant in conditions where tensile failure mechanisms develop, such as the formation of cracks in slopes.

The main contribution of this study is the establishment of a correlation between σ_c and σ_t (Equation 1) for the analyzed soils, supported by both experimental results and numerical modeling. This relationship enables the estimation of tensile strength from commonly obtained compressive strength values, facilitating the incorporation of σ_t into geotechnical analyses when required.

The proposed correlation is applicable to soils with characteristics similar to those studied and should be used with caution for different materials. In such cases, the procedure presented in this study can be followed to obtain an appropriate correlation adapted to the specific soil conditions.

RECOMMENDATIONS

Due to the inherent variability of soils and their dependence on origin and formation conditions, the correlation proposed in this study (Equation 1) is directly applicable to the analyzed soils and to materials with similar characteristics. For soils with different properties, it is recommended to establish a specific correlation between compressive strength (σ_c) and tensile strength (σ_t) based on experimental testing. This involves appropriate field exploration, soil characterization, and the determination of σ_c and σ_t through standardized laboratory tests, followed by regression analysis to define the best-fit relationship between both parameters. In addition, numerical modeling can be used as a complementary approach to evaluate the relationship between σ_c and

σ_t . The use of finite element methods, combined with suitable constitutive models and boundary conditions, allows the simulation of both compressive and tensile tests and provides an alternative means for establishing correlations between these parameters. Alternatively, triaxial modeling may be employed to estimate compressive and tensile strengths under controlled stress conditions, which can also be used to derive σ_c – σ_t relationships consistent with the material behavior.

ACKNOWLEDGMENTS

The authors acknowledge the Soils and Pavements Laboratory, Universidad de Los Andes, Venezuela, and technician Raúl Rivas for their support during testing.

ETHICAL CONSIDERATIONS

This research was conducted in accordance with principles of scientific integrity and laboratory safety. All experimental procedures were performed under controlled conditions, following applicable technical standards and safety protocols to ensure the protection of personnel and the laboratory environment. The study did not involve human participants, animals, or personally identifiable data.

FUNDING

Universidad de Los Andes, Venezuela.

DECLARATION OF COMPETING INTEREST

The authors have declared no conflict of interest

REFERENCES

1. **Briceño Balza JE, Barreto Aldana RC, Guerrero Dávila YL.** Estimation of tensile strength in soils reinforced with synthetic fibers. *Ingenio*. 2025;8(1):43–51. <http://doi.org/10.29166/ingenio.v8i1.7141>
2. **Briceño Balza JE, Castillo Pernía LJ, Mercado Marquez M.** Evaluation of indirect tensile strength and stability of fiber-reinforced cold asphalt mixes. *Ciencia e Ingeniería*. 2025;46(1). <http://erevistas.saber.ula.ve/index.php/cienciaeingenieria/article/view/20611>
3. **Charaja ALA, Mann LAJB.** Improving the mechanical properties of adobe using chilihua fiber and olluco mucilage. *Braz J Dev*. 2025;11(5):e79896. <http://doi.org/10.34117/bjdv11n5-063>
4. **Villalobos Lopez DV.** Effects of the incorporation of coconut fibers on the mechanical properties of adobe [Bachelor's thesis]. Lord of Sipán University; 2025. <http://hdl.handle.net/20.500.12802/15113>
5. **Flores Becerra R.** Study of the mechanical properties of PET fiber-enhanced adobe in the Lambayeque region [Bachelor's thesis]. Universidad Nacional Pedro Ruiz Gallo; 2025. <http://hdl.handle.net/20.500.12893/14614>
6. **Ávila A G.** Tensile strength: study of shrinkage and cracking in clays [Doctoral thesis]. Polytechnic University of Catalunya; 2024. <http://hdl.handle.net/10803/6233>
7. **Zhang L, Wang X, Xia T, Yang B, Yu B.** Deformation characteristics of Tianjiaba landslide induced by surcharge. *ISPRS Int J Geo-Inf*. 2021;10(4):221. <http://doi.org/10.3390/ijgi10040221>

8. **Chen G, Tang P, Huang R.** Critical tension crack depth in rockslides that conform to the three-section mechanism. *Landslides*. 2021;18:79–88. <http://doi.org/10.1007/s10346-020-01471-x>
9. **Tang L, Zhao Z, Luo Z, Sun Y.** What is the role of tensile cracks in cohesive slopes? *J Rock Mech Geotech Eng*. 2019;11:314–324. <http://doi.org/10.1016/j.jrmge.2018.09.007>
10. **Ramírez P, Alejano L.** *Mecánica de rocas: fundamentos e ingeniería de taludes*. Madrid: Red DESIR; 2014.
11. **Abdollahi M, Vahedifard F, Abed M.** Effect of tension crack formation on active earth pressure in unsaturated retaining wall backfills. *J Geotech Geoenviron Eng*. 2021;147(2). [http://doi.org/10.1061/\(ASCE\)GT.1943-5606.0002434](http://doi.org/10.1061/(ASCE)GT.1943-5606.0002434)
12. **Lambe TW, Whitman RV.** *Soil mechanics*. New York: John Wiley & Sons; 1979.
13. **Abu-Hejleh AN, Znidarcic D.** Desiccation theory for soft cohesive soils. *J Geotech Eng*. 1995;121(6):493–502. [http://doi.org/10.1061/\(ASCE\)0733-9410\(1995\)121:6\(493\)](http://doi.org/10.1061/(ASCE)0733-9410(1995)121:6(493)).
14. **Farrell DA, Greacen EL, Larson WE.** The effect of water content on axial strain in a loam soil under tension and compression. *Soil Sci Soc Am J*. 1967;31(4):445–450. <http://doi.org/10.2136/sssaj1967.03615995003100040011x>.
15. **Torres J, Torres R.** Numerical analysis of the direct shear test on silty sands planted with vetiver. In: *Proc 17th PCSMGE*; 2024. http://www.issmge.org/uploads/publications/84/130/FV_404_-_MT_4_-_FV.pdf
16. **Ortiz Morocho KR, Viracucha Llano JX.** Analysis of the ultimate bearing capacity of soil using analytical methods and finite elements. 2025. <http://dspace.ups.edu.ec/handle/123456789/29675>.
17. **Achá M, Moscoso Á, Gonzales G.** Parametric analysis of soil-structure interaction in an isolated foundation by FEM. *Investig Desarro*. 2024;24(1):5–20. <http://doi.org/10.23881/idupbo.024.1-1i>
18. **Segundo J, Quispe S.** Análisis correlacional de presiones admisibles en suelos finos. *CONCYTEC*; 2024. http://alicia.concytec.gob.pe/vufind/Record/UACI_db3075e894276afbe6290ff1980be2d7.
19. **Moreno J.** Ajuste a los parámetros de resistencia de depósitos de coluviones. 2012. <http://repositorio.escuelaing.edu.co/entities/publication/0022beda-79da-439c-a247-dbf09ddad0b0>.
20. **Caro C, Catellet I, Ernest B.** Correlación de parámetros geotécnicos con modelo hidrológico superficial. *Ingenio Magno*. 2013;4:76–86. <http://revistas.santototunja.edu.co/index.php/ingeniomagno/article/view/755/672>
21. **Radelet-de Grave P.** A study of Coulomb's application of the rules of maxima and minima to problems of statics. In: *Radelet-de Grave P. Between mechanics and architecture: the mathematical search for stability in architecture*. Cham: Birkhäuser; 2025. p. 265-298. *Mathematics and the Built Environment*; vol. 8. http://doi.org/10.1007/978-3-031-73530-1_10.
22. **Labuz JF, Zang A.** Mohr–Coulomb failure criterion. *Rock Mech Rock Eng*. 2012;45:975–979. <http://doi.org/10.1007/s00603-012-0281-7>.
23. **Zhang L, Zheng H.** The Cosserat continuum with hyperbolic Mohr–Coulomb surface. *Int J Rock Mech Min Sci*. 2026;199:106425. <http://doi.org/10.1016/j.ijrmms.2026.106425>.
24. **Catari P, Barriga C, Villanueva C, Gómez J, Alvarado H, Melgar D, et al.** Optimización del diseño de talud mediante FEM. *Novasinerгия*. 2025;8(1):33–51. <http://doi.org/10.37135/ns.01.15.09>.

- 25.Vera N, Moreano R, Loayza R.** Aplicación del método de elementos finitos en estabilidad de taludes. Micaela. 2025;6(2):86–94. <http://doi.org/10.57166/micaela.v6.n2.2025.191>.
- 26.Li HD, Tang CS, Cheng Q, Li SJ, Gong XP, Shi B.** Tensile strength of clayey soil. Eng Geol. 2019;253:137–148. <http://doi.org/10.1016/j.enggeo.2019.03.017> .
- 27.Wang R, Li Y, Lv D, Zhao W, Zhang C, Zachert H, et al.** Comparison of test methods for tensile strength of soil. Front Earth Sci. 2022;10:835851. <http://doi.org/10.3389/feart.2022.835851>.
- 28.Guan FF, Li YR, Gao GH, Beroya-Eitner MA, Zachert H.** Horizontal compression test for tensile strength. Front Earth Sci. 2022;10:839073. <http://doi.org/10.3389/feart.2022.839073>